Synthesis and Characterization of Branched Polyelectrolytes. 1. Preparation of Hyperbranched Poly(acrylic acid) via Self-Condensing Atom Transfer Radical Copolymerization

Hideharu Mori, Delphine Chan Seng, Hans Lechner, Mingfu Zhang, and Axel H. E. Müller*

Makromolekulare Chemie II and Bayreuther Zentrum für Kolloide und Grenzflächen, Universität Bayreuth, D-95440 Bayreuth, Germany

Received July 22, 2002; Revised Manuscript Received September 25, 2002

ABSTRACT: We report on the synthesis of randomly branched (arborescent) poly(acrylic acid) (PAA) by self-condensing vinyl copolymerization (SCVCP) of an acrylic AB* inimer, 2-(2-bromopropionyloxy)ethyl acrylate (BPEA), with *tert*-butyl acrylate (tBuA) via atom transfer radical polymerization (ATRP), followed by hydrolysis of *tert*-butyl groups. Depending on the comonomer ratio, $\gamma = [tBuA]_0/[BPEA]_0$, branched PtBuAs with number-average molecular weights between 8000 and 76 000 and degrees of branching (DB) between 0.48 and 0.02 were obtained by SCVCP, as evidenced by GPC, GPC/viscosity, GPC/MALS, and NMR analysis. For the case of high comonomer ratios, $\gamma \gg 1$, the degree of branching is given as DB $\approx 2/(\gamma + 1)$, and γ corresponds to an average number of tBuA units between branch points. The Mark−Houwink exponents of these branched PtBuAs obtained at $\gamma = 0.5-100$ are significantly lower ($\alpha = 0.38-0.47$) than that of linear PtBuA ($\alpha = 0.80$). The nature of the ligand and polymerization temperature affect the molecular weights and chain architectures, while the comonomer-to-catalyst ratio, $\mu = ([tBuA]_0 + [BPEA]_0)/[CuBr]_0$, has a slight influence only on these parameters. Subsequent cleavage of the *tert*-butyl ester moieties by acidic hydrolysis gave randomly branched polyelectrolytes, PAA, as confirmed by elemental analyses, ^{1}H NMR, and FT-IR measurements. Aqueous-phase GPC and dynamic light scattering confirm the compact structure of the branched PAAs. Their water solubility and their size depend on the degree of branching and on pH.

Introduction

In the past decade, the field of hyperbranched and highly branched polymers (arborescent polymer) has been well established with a large variety of synthetic approaches, fundamental studies on structure and properties of these unique materials, and possible applications. Recently, branched polyelectrolytes became of special interest, which are composed of a certain fraction of electrically charged monomers and several branching points. Poly(ethylene imine), which is important in various industrial applications, can provide an excellent example: branched and linear polyelectrolytes have quite different properties.[1] For instance, the former is soluble in water, while the linear one precipitates from aqueous media as various insoluble crystal hydrates in the nonprotonated state. The proton binding characteristics of the linear and branched polyelectrolytes also differ substantially.[2,3] The reason for this different behavior is certainly related to both the different topographies and structures, especially the higher densities of ionizable groups corresponding to the coordination number. Other experimental approaches for characterization and applications of branched polyelectrolytes involve star-shaped[4,5] and cross-linked[6] poly(styrenesulfonate)s, graft copolymers comprising styrene and styrenesulfonate,[7] star and graft polymers containing poly(vinylpyridine),[8−11] and dendritic-like polymers made from a phthalic anhydride/pentaerythritol polycondensation[12] as their salt-free and/or salt forms. A variety of theoretical approaches have been also reported on the investigations of branched polyelectrolytes.[13−18] However, the correlation of the properties and the topology of branched polyelectrolytes is not completely understood, because of difficulties in the synthesis of hyperbranched polymers with well-defined architectures. One challenge in this field is, therefore, to produce randomly or regularly branched polyelectrolytes, which are suitable for various applications as well as for quantitative analysis of the relation between the properties and the architectures. The material properties of branched polymers depend not only on the molecular weight and branching density but also on the type of branching. It is, therefore, desirable to establish precise synthetic methods for various types of branched polymers (random, comb, and star).

We have recently described various approaches for synthesizing novel polyelectrolytes and/or their precursors with defined structures as a step toward the investigation of interesting properties of polyelectrolytes having various branched architectures. A series of star polymers consisting of poly(*tert*-butyl acrylate) (PtBuA) arms and an ethylene glycol dimethacrylate microgel core were synthesized using anionic polymerization.[19] Self-condensing vinyl copolymerization (SCVCP) of an AB* initiator−monomer ("inimer") with *tert*-butyl methacrylate via group-transfer polymerization was utilized to provide a poly(*tert*-butyl methacrylate) having randomly branched structures.[20] Another approach involved the self-condensing vinyl polymerization (SCVP) of a "macroinimer", which is a heterotelechelic PtBuA, possessing both an initiating and a polymerizable moiety, via atom transfer radical polymerization (ATRP).[21] Synthesis of well-defined comb-shaped polymers with PtBuA side chains was conducted by copo-

* Corresponding author: e-mail Axel.Mueller@uni-bayreuth.de.

10.1021/ma021159u CCC: $22.00
Published on Web 11/01/2002

Scheme 1. General Route to Branched Poly(acrylic acid) via Self-Condensing Vinyl Copolymerization, Followed by Hydrolysis

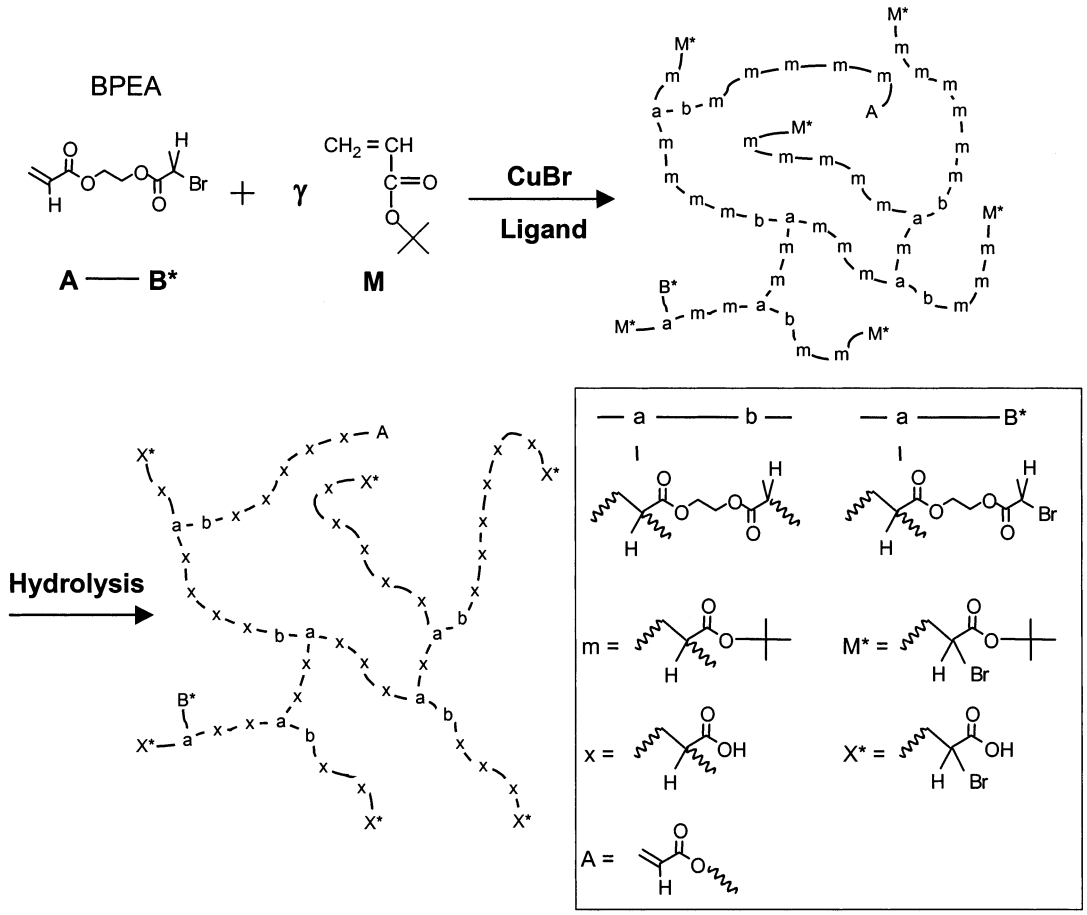

lymerizing with PtBuA macromonomers via ATRP.[22,23] ATRP using the "grafting from" technique was also applied to the preparation of cylindrical brushes with diblock copolymer side chains, one block consisting of PtBuA.[24] Hydrolysis of the *tert*-butyl groups in these polyelectrolyte precursors yields branched architectures involving poly(acrylic acid) (PAA) or poly(methacrylic acid) segments, which should have interesting properties associated with the compact molecular size and the high charge density attainable in these systems. Such branched polymers can exhibit a wide range of solution properties, since the overall nature of a molecule can be changed by judicious control of the branched architecture.

This paper reports on the synthesis of the branched PtBuAs by SCVCP of an acrylic AB* inimer, 2-(2-bromopropionyloxy)ethyl acrylate (BPEA), with tBuA via ATRP using the CuBr/ligand catalyst system. Hydrolysis of the ester functionality in the PtBuA segments creates randomly branched PAAs. The resulting polyelectrolytes with randomly branched structures may behave differently from their star and comb counterparts, even with the same molecular weights and branching density. The synthetic route to branched PAA is outlined in Scheme 1. The curved lines represent polymer chains. A*, B*, and M* are active units, whereas a, b, and m are reacted ones. A is an acryloyl group. X* and x stand for the acrylic acid units at the chain end and in the linear segment, respectively. The great advantages of this method are that the branched polyelectrolytes are synthesized in two steps—(1) SCVCP of an acrylic AB* inimer, BPEA, with tBuA via ATRP and (2) hydrolysis of the *tert*-butyl ester moieties—and the chain architecture can be modified easily by a suitable choice of the comonomer ratio in the feed. The nonionic precursors and ionic final polymer of identical structure can be characterized independently by allowing for the assessment of the effect of charge in the polymer. SCVCP of AB* monomers with conventional monomers (M) allows to control molecular weight distribution and degree of branching.[20,25−27] Further, we have demonstrated that SCVCP in the presence of the functionalized planar silicon surfaces leads to grafted branched polymers, allowing for the control of the film thickness, surface morphology, roughness, and the chemical structure.[28] SCVCP has been also applied for preparation of highly branched polymer—silica nanoparticle hybrids.[29]

In this study, we discuss the resulting randomly branched architecture as a function of the comonomer ratio, $\gamma = [\text{tBuA}]_0/[\text{BPEA}]_0$, and the comonomer-to-catalyst ratio, $\mu = ([\text{tBuA}]_0 + [\text{BPEA}]_0)/[\text{CuBr}]_0$, in the feed. The effects of the ligand used to complex copper ions, solvent, and temperature on the resulting molecular parameters were also studied. Control of the structures of the branched PtBuAs in terms of molecular weight, polydispersity, degree of branching, and comonomer composition plays a crucial role in manipulation of the properties and in further practical application. Branched PAAs obtained after the hydrolysis were characterized by aqueous-phase GPC, potentiometric titration, and DLS.

Experimental Section

Materials. CuBr (95%, Aldrich) was purified by stirring overnight in acetic acid. After filtration, it was washed with ethanol and ether and then dried. *N*,*N*,*N*′,*N*″,*N*″-Pentamethyldiethylenetriamine (PMDETA, 99%, Aldrich) was distilled and degassed. Bipyridine (Bipy) was recrystallized from ethanol to remove impurities. *tert*-Butyl acrylate (tBuA, BASF AG) was fractionated from CaH_2, stirred over CaH_2, and distilled and degassed in high vacuum. Other reagents were commercially obtained and used without further purification. Synthesis of an acrylic AB* inimer, 2-(2-bromopropionyloxy)-ethyl acrylate (BPEA), was conducted by the reaction of an α-bromoacid halide with 2-hydroxyethyl acrylate in the presence of pyridine as reported previously.[28,30] The inimer was degassed by three freeze−thaw cycles.

Polymerization. All copolymerizations were carried out in a round-bottom flask sealed with a plastic cap. A representative example is as follows: BPEA (0.157 g, 0.626 mmol) was added to a round-bottom flask containing CuBr(I) (0.0232 g, 0.162 mmol), PMDETA (0.0280 g, 0.162 mmol), and tBuA (2.00 g, 15.6 mmol). The flask was placed in an oil bath at 60 °C for 4.5 h. Conversion of the double bonds, as detected by ^{1}H NMR, was >95%. Since the reaction was performed in bulk and the conversion was adjusted to reach full conversion, the content of the flask had completely solidified. After the mixture was dissolved in THF and was subsequently passed through a neutral alumina column, GPC measurement was conducted. For GPC/viscosity and NMR measurements as well as the further hydrolysis reaction, the polymer was freeze-dried from benzene and finally dried under vacuum at room temperature. The polymer powder had $M_n = 43\,600$ and $M_w/M_n = 3.32$ (as determined by GPC/viscosity) compared to $M_n = 23\,200$ and $M_w/M_n = 2.88$ (as determined by GPC using linear PtBuA standards).

For the copolymerization in solution, ethyl acetate, *N*,*N*-dimethylformamide (DMF) or acetone (50 vol % to tBuA) was used as a solvent. The monomer conversion was determined by gas chromatography (GC) from the concentration of residual tBuA, using decane as an internal standard (1/10 molar ratio relative to tBuA) in the cases of the polymerization with ethyl acetate and acetone. The copolymerization was also conducted in bulk with CuBr/Bipy system at the ratio of $[CuBr]_0$:$[Bipy]_0$ = 1:3.

A mixture of linear standard PtBuAs with various molecular weights was used as comparison in the solution viscosity studies. Molecular weights for this example: $M_n = 44\,200$ and $M_w/M_n = 2.49$ (determined by GPC/viscosity using universal calibration). Poly(BPEA) obtained by a homo-SCVP was also used for a comparison. The polymer had $M_n = 23\,800$, $M_w/M_n = 2.85$, and $\alpha = 0.36$ (as determined by GPC/viscosity using universal calibration) compared to $M_n = 4600$ and $M_w/M_n = 2.85$ (as determined by GPC using linear polystyrene standards). Fraction of reacted B* units, *b*, determined by ^{1}H NMR was 0.34, corresponding to $DB_{NMR} = 0.43$.

Hydrolysis of Branched Poly(*tert*-butyl acrylate). The branched PtBuA ($\gamma = 10$) (1.5 g, 9.78 mmol ester) was dissolved in dichloromethane (15 mL), and a 5-fold molar excess of trifluoroacetic acid (5.58 g, 48.9 mmol, with respect to the ester groups) was added. The mixture was stirred at room temperature for 24 h. When hydrolyzed, the polymer precipitated in dichloromethane. They were separated by decantation and washed with dichloromethane repeatedly. The resulting polymer was freeze-dried from dioxane containing a small amount of MeOH and finally dried under vacuum at room temperature. The hydrolyzed powders were characterized by FT-IR, ^{1}H NMR in D_2O, CD_3OD, dioxane-d_8, or DMSO-d_6, elemental analyses, and aqueous-phase GPC.

When the branched polymer having lower tBuA content was hydrolyzed, no precipitation of the polymer was observed during the reaction. In these cases, the excess reagents were removed by evaporation under vacuum. The freeze-dry treatment of the resulting polymer was conducted from dioxane or dioxane with MeOH, depending on the solubility of the resulting branched PAAs. For the branched PAAs having higher degree of branching ($\gamma < 3$), viscous honey products were obtained after drying under vacuum at room temperature.

Characterization. Three THF-phase and an aqueous-phase GPC systems were used in this study to characterize branched polymers. The branched PtBuAs obtained by SCVCP were characterized by GPC using THF as eluent at a flow rate of 1.0 mL/min at room temperature. A conventional THF-phase GPC system was used in order to get apparent molecular weights. GPC system I, column set: 5 μm PSS SDV gel, 10^2, 10^3, 10^4, 10^5 Å, 30 cm each; detectors: Waters 410 differential refractometer and Waters photodiode array detector operated at 254 nm. Narrow PtBuA standards (PSS, Mainz) were used for the calibration of the column set I. Molecular weights of the branched polymers were also determined by universal calibration[31] using the viscosity module of the PSS-WinGPC scientific V 6.1 software package. GPC system II; column set: 5 μm PSS SDV gel, 10^3, 10^5, and 10^6 Å, 30 cm each; detectors: Shodex RI-71 refractive index detector; Jasco Uvidec-100-III UV detector ($\lambda = 254$ nm); Viscotek viscosity detector H 502B. GPC-MALS was also performed to determine the true molecular weights of the branched PtBuAs. GPC system III; column set: 5 μm PSS SDV gel, 10^3, 10^5, and 10^6 Å, 30 cm each; detectors: DAWN DSP-F MALS and PSS ScanRef interferometer, both equipped with He−Ne laser (632.8 nm). The interferometer was used to measure the refractive index increment (d*n*/d*c*) online.

The water-soluble branched PAAs obtained after the hydrolysis were analyzed by aqueous-phase GPC at 60 °C using a column set with 8 μm PSS SUPREMA gel, 10^2, 10^3, 10^4 Å, 30 cm each; preceded by a guard column (PSS SUPREMA gel, 8 μm × 5 cm). An aqueous solution of 0.05 M NaN_3 was used as the eluent at a flow rate of 1.0 mL/min. A refractive index detector (Bischoff 8110) and Jasco Uvidec-100-III UV detector ($\lambda = 254$ nm) were used as detectors connected in series. Poly(methacrylic acid) standards (PSS, Mainz) were used for the calibration.

The potentiometric titration was performed using a Schott CG840 pH meter equipped with a glass electrode. The reference electrode was calibrated with buffer solutions of pH 4, 7, and 10 prior to pH measurements. A 25 mL aqueous solution of polymer (1 mg/mL) was titrated with a 0.01 M NaOH standard solution at room temperature, maintained nearly constant at 25 °C. The solution was equilibrated until each pH reading reaches a constant value. The degree of ionization of each sample was calculated as the number of NaOH equivalents added divided by the number of AA equivalents in the sample. The effective p*K* of each sample was estimated as the pH at 50% ionization.

Dynamic light scattering (DLS) was performed at room temperature on an ALV DLS/SLS-SP 5022F compact goniometer system with a He−Ne laser ($\lambda_0 = 632.8$ nm) using an ALV 5000/E correlator. Sample solutions for DLS were prepared as follows: A polymer sample obtained by the hydrolysis was dissolved in water containing 0.1 M NaCl with the concentration of 2.0 mg/mL. The pH value of the solution was adjusted by adding a proper amount of aqueous solution of NaOH or HCl, and the solutions were allowed to stand for 1 day for equilibration. Sample solutions were filtered using Millipore Teflon filters with a pore size of 0.45 μm into dust-free cylindrical cuvettes prior to measurement. The intensity weighted decay time distribution was obtained by CONTIN analysis of the autocorrelation functions. Then under the assumption that the scattering particles behave as hard spheres in dilute solution and within the Rayleigh−Debye theory the particle radius distribution function is calculated from the decay time distribution function using the Stokes−Einstein equation. After measurements at four different angles (30°, 60°, 90°, 120°), the hydrodynamic radius of the species was obtained by extrapolation to $q^2 \rightarrow 0$.

^{1}H NMR spectra were recorded with a Bruker AC-250. FT-IR spectra were recorded on a Bruker Equinox 55 spectrometer. The elemental analyses were performed by Ilse Beetz Mikroanalytisches Laboratorium (Kulmbach).

Table 1. Self-Condensing Vinyl Copolymerization of BPEA and tBuA at Different Comonomer Ratios, γ[a]

entry	γ[b]	$M_{n,GPC}$[c] (M_w/M_n)	$M_{n,GPC-VISCO}$ (M_w/M_n)	α[d]	BPEA ratio in polymer[e]	b[f]	DB_{NMR}[g]	DB_{theo}[h]
1	0.5	4700 (6.59)	16300 (6.24)	0.38	65	0.61	0.48	0.50
2	1.1	4800 (4.29)	8300 (5.41)	0.39	47	0.62	0.42	0.49
3	1.5	4700 (4.95)	12500 (4.62)	0.40	38	0.74	0.42	0.47
4	2.5	5900 (4.44)	13000 (5.93)	0.42	27	0.78	0.35	0.40
5	6.1	8100 (4.36)	16800 (5.41)	0.47	14			0.24
6	10	8400 (3.54)	22700 (3.52)	0.46	10			0.17
			21000 (2.05)[i]					
7	25	23200 (2.88)	43600 (3.32)	0.46	3.2			0.08
			43100 (1.79)[i]					
8	50	37400 (2.63)	48700 (4.01)	0.47	1.6			0.04
9	75	57600 (3.39)	62400 (4.63)	0.46				0.03
10	100	61600 (3.53)	76000 (4.51)	0.47				0.02
			74000 (2.38)[i]					

[a] Bulk polymerization at 60 °C with CuBr/PMDETA at a constant comonomer-to-catalyst ratio, $\mu = [tBuA]_0 + [BPEA]_0)/[CuBr]_0 = 100-110$. Full conversion was reached after 2−5 h. [b] $\gamma = [tBuA]_0/[BPEA]_0$. [c] Calibrated against PtBuA standards. [d] Mark−Houwink exponent as determined by GPC/viscosity measurement. [e] Determined by ^{1}H NMR. [f] Fraction of reacted B* units as determined by ^{1}H NMR. [g] Degree of branching as determined by ^{1}H NMR using eq 1. [h] Theoretical degree of branching as determined using eq 2. [i] MALS results.

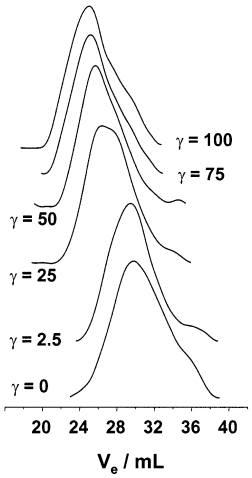

Figure 1. GPC traces of branched copolymers obtained by SCVCP of BPEA and tBuA at different comonomer ratios, $\gamma = [tBuA]_0/[BPEA]_0$.

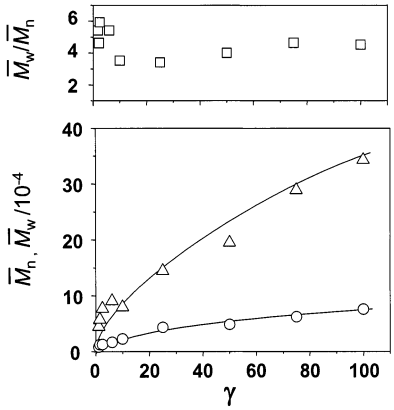

Figure 2. Dependence of molecular weights and polydispersity on the comonomer ratio, $\gamma = [tBuA]_0/[BPEA]_0$: M_n (○), M_w (△), and M_w/M_n (□) as determined by GPC/viscosity using universal calibration.

Results and Discussion

Effect of the Comonomer Ratio. The bulk copolymerization of the AB* inimer, 2-(2-bromopropionyloxy)ethyl acrylate (BPEA), with tBuA was conducted with CuBr/PMDETA at 60 °C at different comonomer ratios, $\gamma = [tBuA]_0/[BPEA]_0$ between 0.5 and 100, keeping the comonomer-to-catalyst ratio at a constant value of $\mu = ([tBuA]_0 + [BPEA]_0)/[CuBr]_0 = 100-110$. Under that condition, full conversion was reached after 2−5 h. The molecular weights and molecular weight distribution (MWD) of the copolymers were characterized by THF-phase GPC using PtBuA standards; the GPC traces are shown in Figure 1. All samples show broad MWDs. The elution curves shift toward higher molecular weights with increasing comonomer ratio, γ. Both number- and weight-average molecular weights of the copolymers consistently increase with γ, whereas the polydispersity index, M_w/M_n, is constant.

As the relation between molecular weight and hydrodynamic volume of branched polymers differs substantially from linear ones, the molecular weights were established by GPC/viscosity using universal calibration. The results are given in Table 1. Depending on the comonomer ratio, γ, molecular weights up to $M_{n,GPC-VISCO} = 76\,000$ at a polydispersity of $M_w/M_{n,GPC-VISCO} =$ ca. 4.5 could be obtained. In this system, the polymerization was conducted until the reaction mixture had solidified completely. According to theory (assuming equal reactivity of active centers[27]), the number-average degree of polymerization, P_n, increases drastically with conversion of the comonomer, x_M, and the polydispersity index, M_w/M_n, decreases with γ. For example, in the case of $\gamma = 100$ and $x_M = 95\%$, $P_n = 1900$ and $M_w/M_n = 20$. The molecular weight and the molecular weight distribution obtained experimentally were lower than the calculated ones. The observation of finite molecular weight averages can be explained by the occurrence of the cyclization reaction, in which an active center reacts intramolecularly with the double bond, forming a polyinitiator containing one loop. Clearly, this loop should only have a minor effect on the physical properties, but its presence limits the molecular weights of branched polymers obtained by SCVCP as well as SCVP and narrows the molecular weight distribution.[20]

Figure 2 represents dependences of polydispersity and average molecular weights on the comonomer ratio in the range of $100 > \gamma > 1$. The number- and weight-average molecular weights of the copolymers as determined by GPC−viscosity by universal calibration consistently increase with γ, whereas there is no significant difference in the polydispersity at $\gamma > 10$. The variation in the molecular weights is in qualitative agreement with the assumption that a relationship between γ and molecular weights should be linear when the ratio of

reaction rates of cyclization and chain propagation is independent of comonomer ratio, γ.[20] In all samples, as can be compared in Table 1, the molecular weights determined by GPC−viscosity are higher than apparent ones obtained by GPC, indicating highly branched structures. For $10 \geq \gamma \geq 1.1$, the ratios of $M_{n,GPC-VISCO}$ to $M_{n,GPC}$ of the copolymers are 1.7−2.7, while smaller ratios (1.1−1.8) are observed in the cases of $\gamma \geq 25$. It means that a suitable amount of AB* inimer, BPEA, in the feed considerably leads to a compact structure, and the difference in the amount has an influence on the molecular weights and compact structure in solution. For lowest γ value ($\gamma = 0.5$), the molecular weight determined by GPC−viscosity is higher than that in the case of $\gamma = 1.1$, while it is lower than that of a hyperbranched poly(BPEA) obtained by a homo-SCVP. The ratio of $M_{n,GPC-VISCO}$ to $M_{n,GPC}$ (3.5) is also in between the values for hyperbranched poly(BPEA) (5.2) and the branched PtBuA (1.7 at $\gamma = 1.1$). GPC-MALS (multiangle light scattering) was also applied for the determination of the absolute molecular weights. Here, it is necessary to take into account the influence of the refractive index increment, d*n*/d*c*, in the low-γ region, because the different comonomer compositions may affect the value of d*n*/d*c*, leading to deviation of the absolute molecular weights. A good agreements between $M_{n,GPC-VISCO}$ and $M_{n,GPC-MALS}$ is observed in the cases of $\gamma \geq 10$, as can be seen in Table 1. Note that the true M_n of copolymer is obtained by GPC-MALS even if the composition and therefore the refractive index increment vary with elution volume, whereas M_w determined by GPC-MALS is affected by d*n*/d*c* and is only an apparent value.[32] As for the branched polymers with lower comonomer composition, $\gamma < 10$; unfortunately, no reliable light scattering data could be obtained because of low signal-to-noise ratio originating from the low refractive index increment of the branched PtBuAs as well as low molecular weights.

Relationships between dilute solution viscosity and molecular weight have been determined for many hyperbranched systems, and the Mark−Houwink constant typically varies between 0.5 and 0.2, depending on the degree of branching. In contrast, the exponent is typically in the region of 0.6−0.8 for linear homopolymers in a good solvent with a random coil conformation. The contraction factor,[33] $g' = [\eta]_{branched}/[\eta]_{linear}$, is another way of expressing the compact structure of a branched polymers. Experimentally, g' is computed from the intrinsic viscosity ratio at constant molecular weight. The contraction factor can be expressed as the averaged value over the molecular weight distribution or as a continuous fraction of molecular weight. Figures 3 and 4 show the Mark−Houwink plots and contraction factors as a function of the molecular weight for representative branched polymers obtained by SCVCP. Plots of a hyperbranched polymer obtained by homo-SCVP of BPEA and a linear PtBuA are shown as comparisons. The viscosities of the branched PtBuAs are significantly less than that of the linear PtBuA and decrease with $1/\gamma$. At higher molecular weights (log M > 5.0), the intrinsic viscosity of the branched PtBuA ($\gamma = 25$) is less than 70% of that of the linear one. The contraction factors for all the branched polymers decrease with increasing molecular weights, as shown in Figure 4, indicating a highly compact structure in solution. There are only slight difference in the slopes between the branched copolymers, but the values at each molecular

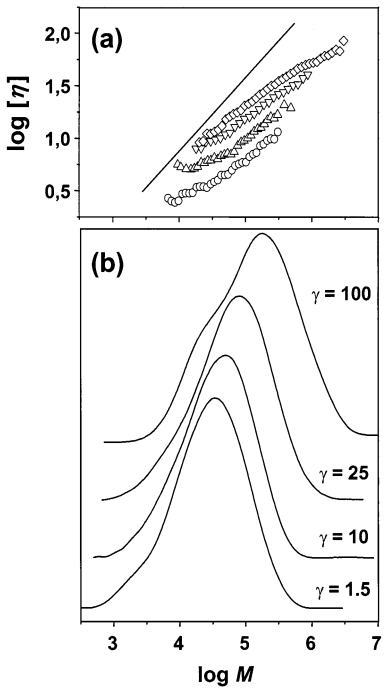

Figure 3. Mark−Houwink plots (a) and RI signals (b) for the polymers obtained by copolymerizations of BPEA and tBuA: $\gamma = 1.5$ (○), 10 (△), 25 (▽), and 100 (◇). Samples: see Table 1. The intrinsic viscosity of a linear PtBuA (—) is given for comparison.

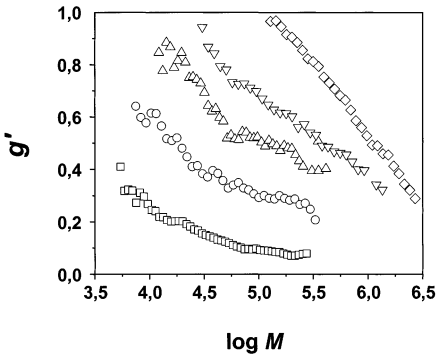

Figure 4. Contraction factors, $g' = [\eta]_{branched}/[\eta]_{linear}$, for the polymers obtained by SCVP of BPEA (□) and by copolymerizations: $\gamma = [tBuA]_0/[BPEA]_0 = 1.5$ (○), 10 (△), 25 (▽), and 100 (◇). Samples: see Table 1.

weight increase obviously with increasing γ value. These results indicate that the apparent discrepancy between molecular weights determined from GPC/viscosity compared to conventional GPC arises from a systematic decrease in Mark−Houwink exponent, α, and the contraction factor, g', resulting from a more compact architecture with an increased number of branches.

Figure 5 shows the influence of the comonomer ratio, γ, on the Mark−Houwink exponent. In the whole range of γ values, the exponents of the branched polymers are significantly lower ($\alpha = 0.38-0.47$) compared to that for linear PtBuA ($\alpha = 0.80$). Particularly, the branched PtBuAs obtained at lower γ value ($\gamma < 10$) show values comparable to that of a hyperbranched poly(BPEA) ($\alpha = 0.36$) obtained by a homo-SCVP. The values obtained at $\gamma = 10-100$ are comparable to that of the branched PtBuA obtained by a SCVP of a PtBuA macroinimer via ATRP ($\alpha = 0.47$).[21] At a comonomer ratio of $\gamma = 100$ (corresponding to only 1% inimer), the α value is still only 50−60% of the value of linear PtBuA. This is an

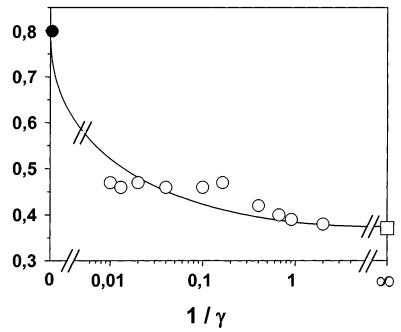

Figure 5. Dependence of the Mark−Houwink exponent, α, on comonomer ratio, γ (○). Linear PtBuA (●): α = 0.80. Hyperbranched poly(BPEA) (□): α = 0.36.

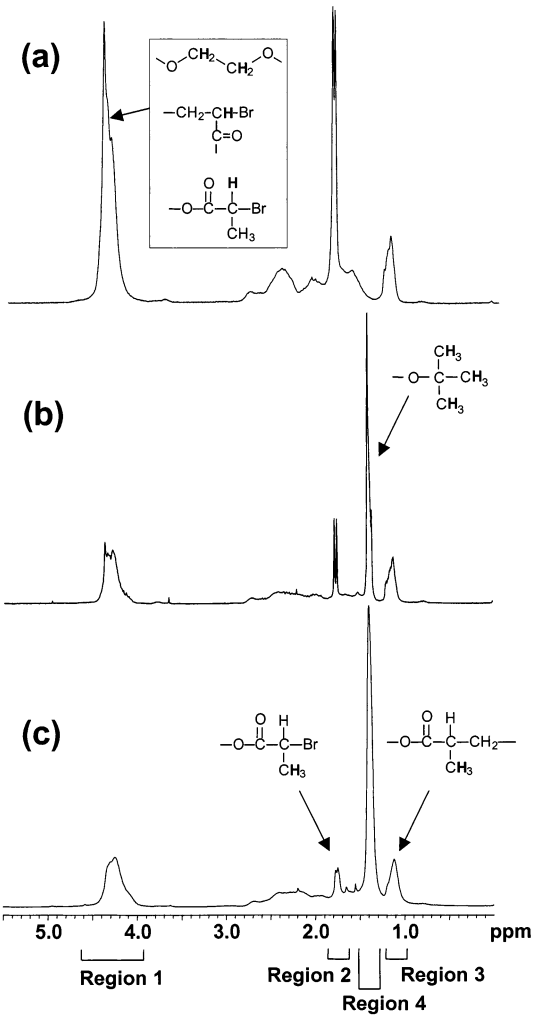

Figure 6. ^{1}H NMR spectra in $CDCl_3$ of the polymers obtained by SCVP of BPEA (a) and by copolymerizations of BPEA and tBuA: γ = 0.5 (b), γ = 1.1 (c).

indication that the branching structure induced by the copolymerization with a tiny amount of AB* inimer has significant influence on macroscopic quantities such as intrinsic viscosity and radius of gyration, even if the degrees of branching of the copolymers are expected to be lower than that of the corresponding hyperbranched polymers obtained by homo-SCVP.

Degree of Branching. Figure 6 shows the respective ^{1}H NMR spectra of the branched PtBuAs obtained by SCVCP and a poly(BPEA) obtained by a homo-SCVP of BPEA. The broad peak of region 1 corresponds to the protons of the ethylene linkage and the protons which are geminal to bromine in either A*, B*, or M*, all of which are derived from BPEA. The later protons correspond to the end groups. Although B* in BPEA is consumed during the copolymerization, for every B* consumed one A* or M* is formed, and consequently, original B* = B^*_{left} + A* + M*. Hence, the sum of protons of the ethylene linkage and geminal to bromine is proportional to the fraction of BPEA in the copolymer but independent of the degree of branching. The peak at 1.3−1.4 ppm, region 4, is assigned to the *tert*-butyl group of PtBuA segment. The comonomer composition calculated from the ratio of these peaks is in good agreement with the comonomer composition in the feed which corresponds to the γ value, as can be seen in Table 1. The agreement demonstrates complete inimer incorporation. The broad peaks at 1.2−2.8 ppm are attributed to the backbone (methylene and methine protons). The large doublet at 1.85 ppm, region 2, is assigned to CH_3 of the 2-bromopropionyloxy group, B* (corresponding to an end group), while the broad peak at 1.0−1.3 ppm, region 3, is assigned to b, which is formed by activation of the B* and subsequent addition of monomer. In the case of poly(BPEA), the proportions of b and B* can be calculated from these peaks.[28,34−36] For the copolymer obtained by SCVCP, these peaks should be related to the degree of branching and the comonomer composition. The proportion of b calculated by the equation b = (region 3)/(sum of region 2 and region 3) was 0.62 in the case of copolymerization at γ = 1.1. For equal reactivity of active sites, the degree of branching determined by NMR, DB_{NMR}, at full conversion is given as[20]

$$DB_{NMR} = 2\left(\frac{b}{\gamma + 1}\right)\left[1 - \left(\frac{b}{\gamma + 1}\right)\right] \qquad (1)$$

According to the theory of SCVCP, the comonomer ratio, γ, can be directly related to the degree of branching.[27] Assuming equal reactivity of all active sites, the degree of branching obtained from the theory, DB_{theo}, at full conversion can be represented as

$$DB_{theo} = \frac{2(1 - e^{-(\gamma+1)})(\gamma + e^{-(\gamma+1)})}{(\gamma + 1)^2} \qquad (2)$$

From these approaches, DB_{NMR} = 0.42 and DB_{theo} = 0.49 can be obtained at γ = 1.1 (b = 0.62). Note that these values represent a rough estimate, as they are calculated on the basis of the assumption of equal rate constants for copolymerization. For low γ value (γ = 0.5), the degree of branching (DB_{NMR} = 0.48) even exceeds the value for poly(BPEA) (DB_{NMR} = 0.43) obtained by a homo-SCVP. This is in accordance with the theoretical prediction that a maximum of DB = 0.5 is reached at γ = 0.6.[27] The effect can be explained by the addition of monomer molecules to in-chain active centers (i.e., in linear segments), leading to very short branches. For 2.5 ≥ γ ≥ 0.5, DB_{NMR} decreases with γ, as predicted by calculations. In all cases, however, the observed values are slightly lower than the calculated ones, which might be attribute to the simplifications made for calculations.

Although NMR experiments afford a conclusive measurement of the degree of branching for lower γ value, the low concentration of branch points in the copolymer at γ > 6 does not permit the determination of the degree of branching directly by the spectroscopic method, because of low intensities of the peaks in regions 2 and

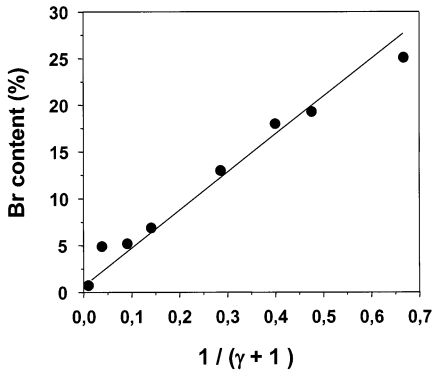

Figure 7. Dependence of bromine content on $1/(\gamma + 1)$. Samples: see Table 1. The calculated value (—) is given for comparison.

3, as shown in Figure 9a. However, for the case of high comonomer ratios, $\gamma \gg 1$, the relation between DB_{theo} and γ becomes very simple and does not depend on the reactivity ratios of the various active centers. It is represented as $DB_{theo} \approx 2/(\gamma + 1)$. In the case of $\gamma = 25$, theory predicts $DB_{theo} = 0.077$. We calculated a fraction of branched units $f_B = DB_{theo}/2 = 0.038$, i.e., which corresponds to 38 branching points in 1000 monomer units or an average of 25 monomer units between branch points. In this copolymerization system, BPEA used as an AB* inimer contains the acrylate and bromopropionate groups, both of which form secondary radicals, and tBuA used as a comonomer also generates a secondary radical. The secondary α-bromoester dormant species formed during the reaction should have a reactivity similar to the 2-bromopropionate found on the AB* inimer. Hence, the difference in the rate constants for the six possible propagation reactions of the different centers is considered to be small. However, a slow deactivation of the propagating radicals was shown to lead faster apparent reactivity ratios (see below). When the reactivities of the various active centers are not equal, the dependences are more complex, and the degree of branching may be higher or lower, depending upon the systems.

With ATRP, nearly every chain should contain a halogen atom at its end group, if termination and transfer are essentially absent. This halogen atom can be replaced through a variety of reactions leading to end-functional polymers and used as the initiating part for polymerization of a second monomer. Halogen atom displacement reactions from hyperbranched polystyrene and polyacrylate have also been reported.[37,38] Hyperbranched polymers can further initiate polymerizations forming hyperstar (dendrigraft) polymers.[39] In the case of ideal SCVCP via ATRP, the resulting branched polymers carry one bromoester function per inimer unit, and the functionality decreases with comonomer (tBuA) composition. As can be seen in Figure 7, the bromine contents of the branched polymers are dependent upon the comonomer composition in the feed and are in good agreement with the calculated values. This is an indication that unfavorable termination and transfer reactions are essentially negligible under the condition used in this study, and the number of bromoester end groups can be simply determined by the comonomer ratio, γ, in the feed.

Effect of the Comonomer-to-Catalyst Ratio. In a homo-SCVP via ATRP, the catalyst concentration is one of the key factors to control the topological structures as well as the molecular parameters. For example, the significant influence of catalyst-to-inimer ratio on SCVP of 4-(chloromethyl)styrene with CuCl/2,2′-dipyridyl has been reported by Weimer et al.[38] They demonstrated that the resulting polymer is largely linear at low catalyst-to-inimer ratio, while the higher ratio favors the formation of a branched structures. In a previous paper,[28] we also demonstrated that the degree of branching and molecular weight of soluble poly(BPEA) obtained by a homo-SCVP decreased with increasing $[BPEA]_0$:$[CuBr]_0$ ratio. In the presence of larger amounts of the catalyst, generally more deactivator is formed, allowing for faster deactivation and for a more random initiation from the various alkyl halide species in the macromolecules, which lead to higher branching. At the same time, in the presence of more catalyst, more radicals are also formed, leading to more termination. On the other hand, less amounts of catalyst are preferable for practical applications and industrial large scale productions. To find the optimal catalyst concentration, the copolymerization behavior was investigated in terms of the comonomer-to-catalyst ratio. A comonomer-to-catalyst ratio is expressed as $\mu = ([tBuA]_0 + [BPEA]_0)/[CuBr]_0$, where $[tBuA]_0$, $[BPEA]_0$, and $[CuBr]_0$ represent the initial concentration of comonomer, inimer, and catalyst, respectively. The bulk copolymerization of BPEA with tBuA was conducted with CuBr/PMDETA at 60 °C at different comonomer-to-catalyst ratios, $\mu = 25-300$, and a constant comonomer ratio, $\gamma = 25$. The conditions for the copolymerizations were adjusted to yield polymers quantitatively (conversion determined by ^{1}H NMR was >85% in all cases). The results are given in Table 2. In all cases, the molecular weights ($M_{n,GPC-VISCO} = 26\,400-43\,600$) determined by GPC−viscosity are much higher than the corresponding apparent ones, indicating a lower hydrodynamic volume of the branched polymers. The ratio μ has a slight effect only on the molecular weights and the polydispersity of the branched PtBuAs. The corresponding Mark−Houwink plots show that all branched polymers have lower viscosities than linear PtBuA. There are no significant differences in the Mark−Houwink exponent, α, for different comonomer-to-catalyst ratios, μ. These results suggest that the range of the comonomer-to-catalyst ratio used in this study ($\mu = 25-300$) favors the formation of the branched structures, and the resulting degree of branching has enough effect on the improvement in the solution viscosity. When the polymerization was conducted at a very low catalyst concentration ($\mu = 400$), the fluid reaction mixture did not solidify and only oligomer ($M_{n,GPC-VISCO}$ = ca. 2000) was obtained even after 96 h.

Table 2. Effect of Comonomer-to-Catalyst Ratio in Self-Condensing Vinyl Copolymerization of BPEA and tBuA at $\gamma = 25$[a]

μ[b]	time (h)	$M_{n,GPC}$[c] (M_w/M_n)	$M_{n,GPC-VISCO}$ (M_w/M_n)	α[d]
26	4.5	19800 (3.94)	31700 (4.01)	0.46
50	4.5	20200 (3.54)	31600 (4.65)	0.46
100	4.5	23200 (2.88)	43600 (3.32)	0.46
150	24	21000 (4.04)	35700 (4.44)	0.45
300	24	18100 (4.32)	26400 (4.47)	0.45
400	96[e]	2000 (2.04)	2300 (3.22)	

[a] Bulk polymerization at 60 °C with CuBr/PMDETA at a constant comonomer ratio, $\gamma = [tBuA]_0/[BPEA]_0 = 25$. Conversion of double bonds as determined by ^{1}H NMR > 85%. [b] $\mu = ([tBuA]_0 + [BPEA]_0)/[CuBr]_0$. [c] Calibrated against PtBuA standards. [d] Mark−Houwink exponent as determined by GPC/viscosity measurement. [e] Conversion = 80%.

Table 3. Self-Condensing Vinyl Copolymerization of BPEA and tBuA at $\gamma = 25$ under Various Reaction Conditions[a]

ligand[b]	solvent	temp (°C)	time (h)	conv[c] (%)	$M_{n,GPC}$[d] (M_w/M_n)	$M_{n,GPC-VISCO}$ (M_w/M_n)	α[e]
PMDETA		30	4.5	91	23100 (3.77)	35000 (4.02)	0.71
		60	4.5	95	23200 (2.88)	43600 (3.32)	0.46
		100	1	86	12300 (5.57)[h]	23500 (4.24)[h]	0.59[h]
	EAc[f]	60	24	>99[g]	13100 (3.72)	25000 (2.98)	0.51
	acetone[f]	40	24	93[g]	8700 (2.40)	14200 (2.26)	0.46
	DMF[f]	60	24	>99	13200 (3.42)	22300 (3.94)	0.49
Bipy		60	4.5	86	376000 (3.01)[h]	403000 (3.45)[h]	0.56[h]
		100	2	81	74900 (4.75)	92300 (5.35)	0.50

[a] Copolymerization with CuBr at a constant comonomer ratio, $\gamma = [tBuA]_0/[BPEA]_0 = 25$, and a constant catalyst concentration, $\mu = ([tBuA]_0 + [BPEA]_0)/[CuBr]_0 = 100$. [b] PMDETA (*N*,*N*′,*N*″,*N*″-pentamethyldiethylenetriamine) or Bipy (bipyridine) was used as a ligand. [c] Conversion of double bonds as determined by ^{1}H NMR. [d] Calibrated against PtBuA standards. [e] Mark−Houwink exponent as determined by GPC/viscosity measurement. [f] Ethyl acetate, acetone, or *N*,*N*-dimethylformamide (50 vol % to tBuA) was used as a solvent. [g] Conversion of tBuA determined by GC. [h] Results obtained from THF-soluble parts.

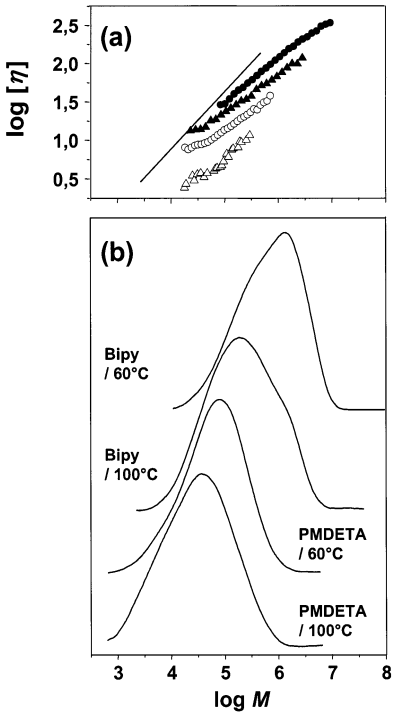

Figure 8. Mark−Houwink plots (a) and RI signals for the polymers obtained by copolymerizations; CuBr/PMDETA at 60 °C (○) and 100 °C (△); CuBr/Bipy at 60 °C (●) and 100 °C (▲). Samples: see Table 3. The viscosity result for a linear PtBuA (—) is given for comparison.

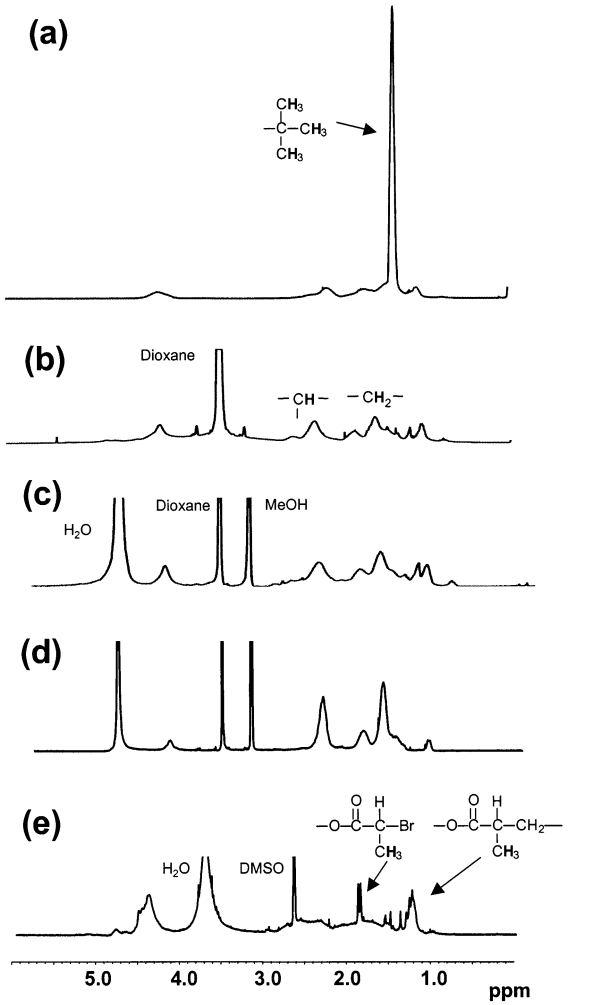

Figure 9. ^{1}H NMR spectrum of branched PtBuA, $\gamma = 6.1$, $CDCl_3$ (a). ^{1}H NMR spectra of branched PAA, $\gamma = 6.1$, 1,4-dioxane-d_8 (b), $\gamma = 6.1$, CD_3OD (c), $\gamma = 25$, CD_3OD (d), and $\gamma = 1.1$, DMSO-d_6 (e).

Effect of the Polymerization Conditions. Here, we investigated the influence of the various factors (the ligand used to complex copper ions, solvent, and temperature) on the architectures of the branched PtBuAs. Table 3 summarizes the conditions and the results of the copolymerization under various conditions. In all cases, the copolymerization of BPEA with tBuA was conducted with CuBr at a constant comonomer-to-catalyst ratio, $\mu = 100$, and a constant comonomer ratio, $\gamma = 25$. Comparisons of the Mark−Houwink plots and RI signals for the representative polymers obtained are shown in Figure 8.

When the polymerization was conducted with CuBr/PMDETA at 30 and 60 °C, the characteristic green color kept constant during the polymerization, and the content of the flask had completely solidified after 1−3 h. In contrast, the reaction medium turned from green to dark brown rapidly after heating to 100 °C, and it solidified after 15 min. In this case, ca. 30 wt % of insoluble product was obtained. An apparent lowering of molecular weights at higher polymerization temperature is caused by a loss of the high molecular weight fraction from the whole solution as some molecules reach the gel point at the onset of cross-linking. On the other hand, the copolymerization at lower temperature (30 °C) gave a polymer having a higher Mark−Houwink exponent, suggesting a lower degree of the branching. When the polymerization was conducted in ethyl acetate (50 vol % to tBuA), the viscous reaction mixture did not solidify even after the conversion of tBuA reached more than 95%. However, usage of ethyl acetate as a polymerization solvent led to a decrease in the molecular weights. The copolymerizatios with other solvents (DMF and acetone) also showed the same tendency.

The copolymerization with the CuBr/Bipy catalyst system at 60 and 100 °C gave polymers having higher molecular weights. In both cases, the dark brown reaction media solidified at the end of the polymerization. An insoluble product was obtained at 60 °C, and the polymer yield of the soluble part after the column purification was about 60%. The increase in the polymerization temperature led to a decrease in the apparent molecular weights of the products. The higher molecular weights may be attributed to slow deactivation of the propagating radicals. The formation of insoluble material is likely the results of cross-linking process derived from radical−radical combination.

The significant influence of solubility of the deactivator and of the polymerization temperature, which are closely related to the concentration of Cu(II), on the topology of the resulting polymers has been reported in the homo-SCVP of BPEA.[40] For example, it was demonstrated that the polymerization catalyzed by CuBr/Bipy at 50 °C provided essentially a linear polymer, while the degree of branching was observed to increase with temperature and a highly branched poly(BPEA) (DB = 0.46) was obtained at 100 °C. When ATRP is used to prepare linear chains, the activation of the bromoester, and subsequent polymerization, is usually slow due to the low initiator concentration (0.1 M), as compared to homo-SCVP (bulk, ∼10 M). Because the initial rate of radical formation is faster in homo-SCVP, the concentration of radicals is higher, leading to an increased amount of termination. Hence, a higher proportion of Cu(II) is required to lower the concentration of radicals in the polymerization system. On the other hand, the polymerization becomes extremely slow when the proportion of Cu(II) relative to Cu(I) is too high. The concentration of the bromoester during SCVCP is basically dependent upon the comonomer ratio, γ, in the feed, and the initial rate of radical formation should be slower than in the synthesis of highly branched poly(BPEA) by homo-SCVP. The difference in the molecular weights of the products obtained from SCVCP with CuBr/PMDETA and CuBr/Bipy may be attributed to the Cu(I)/Cu(II) ratio, which is related closely to the equilibrium between the active and dormant species in the system.

Hydrolysis of Branched Poly(*tert*-butyl acrylate). The *tert*-butyl ester groups in the branched PtBuAs were hydrolyzed using 5-fold molar excess of trifluoroacetic acid in dichloromethane at room temperature for 24 h. The resulting branched PAA (γ = 6.1) in the acid form is directly soluble in water, as well as in methanol or dioxane, while insoluble in dichloromethane. As shown in Figure 9, the hydrolyzed sample in dioxane-d_8 shows the complete disappearance of the *tert*-butyl resonance at 1.4 ppm and reveals resonances at 0.9−3.0 ppm, corresponding to the backbone protons. The missing resonance of the *tert*-butyl groups in CD_3OD as well as in dioxane-d_8 clearly indicates the quantitative hydrolysis of ester functionality. The complete hydrolysis was also confirmed by ^{1}H NMR measurement in D_2O and DMSO-d_6. It is important to note that the unchanged resonance signal of protons of the ethylene linkage and those geminal to bromine at 4.0−4.6 ppm, suggesting that the BPEA composition in the branched PAA is almost the same to that in branched PtBuA. The complete disappearance of the *tert*-butyl resonance at 1.4 ppm and clear peaks attributed to the backbone are also seen in the branched PAA (γ = 25) in CD_3OD. The spectrum also reveals a relatively lower intensity of the peak at 4.0−4.6 ppm compared to the intensities of the backbone peaks which is due to the higher γ value. The ^{1}H NMR of the branched PAA having higher branching points (γ = 1.1, Figure 9e) in DMSO-d_6 reveals peaks at 1.85 and 1.0−1.3 ppm, which are assigned to CH_3 of the 2-bromopropionyloxy group, B*, and assigned to b, respectively. The proportion of *b* calculated by the ratio of these peaks is 0.64, which is in good agreement with that of the original branched PtBuA (b = 0.62, γ = 1.1). The fractions of the reacted B* in the branched PAAs having different γ values, as determined by ^{1}H NMR in DMSO-d_6, are as follows: b = 0.57 (γ = 0.5), 0.72 (γ = 1.5), and 0.76 (γ = 2.5), which are also consistent with the values before the hydrolysis (see Table 1). These results indicate that the branched structure is intact during the complete hydrolysis of the *tert*-butyl ester groups.

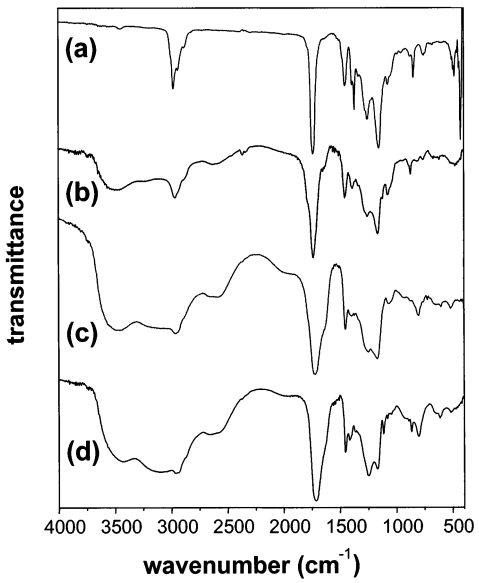

Figure 10. FT-IR spectra of (a) branched PtBuA (γ = 1.1), (b) branched PAA (γ = 1.1), (c) branched PAA (γ = 6.1), and (d) linear PAA.

Figure 10 shows the FT-IR spectra of the branched PtBuAs before and after hydrolysis. The spectrum of the branched PtBuA (γ = 1.1) is characterized by the C−H stretching vibration between 2840 and 2940 cm^{-1} and by the strong C═O vibration at 1735 cm^{-1}. After hydrolysis, the acid functionality is clearly visible as the broad absorption from 2400 to 3800 cm^{-1}. A broader carbonyl vibration is also observed, which may be due to the overlap of the ester groups in the branching points and the carboxylic acid groups obtained after hydrolysis. Furthermore, there is a clear peak between 2840 and 2940 cm^{-1} which is due to the C−H stretching vibration in the main chain and BPEA units acting as branching points. The spectrum of the branched PAA (γ = 6.1) clearly reveals the carbonyl stretch vibration (1725 cm^{-1}) corresponding to free carbonyl bond and a shoulder on the lower wavenumbers (1640 cm^{-1}) which is due to hydrogen−carboxy bonded carbonyl groups, in addition to the acid functionality observed between 2300 and 3800 cm^{-1}. The spectrum of the branched PAA having lower branching points is almost the same as that of linear PAA, which is characterized by the broad absorption from 2300 to 3800 cm^{-1}and the strong C═O vibrations at 1715 and 1640 cm^{-1}.

The hydrolysis was also confirmed by elemental analysis. For example, the atomic composition of the hydrolyzed branched copolymer ($\gamma = 10$) was C, 46.8; H, 5.3; Br, 8.2 (calcd: C, 47.0; H, 5.3; Br, 8.2), while the value of the same sample before the hydrolysis was C, 61.3; H, 8.7; Br, 5.2 (calcd: C, 61.1; H, 8.6; Br, 5.2). The bromine contents of the representative branched PAAs (1.0% for $\gamma = 100$, 3.6% for $\gamma = 25$, 10.7% for $\gamma = 6.1$, and 24.6% for $\gamma = 0.5$) were also in agreement with the calculated values (1.1% for $\gamma = 100$, 3.9% for $\gamma = 25$, 11.6% for $\gamma = 6.1$, and 27.9% for $\gamma = 0.5$). The reasonable bromine content of the hydrolyzed product indicates that most of the terminal bromoester groups are kept without any modification during the hydrolysis reaction and can be used for further modifications. To prove the stability of the branched structures under the hydrolysis condition, a control experiment was conducted with a poly(BPEA) prepared independently by a homo-SCVP of BPEA. The branching structures of the poly(BPEA) are the same as that of the branched PtBuA obtained by SCVCP, but the number of the branch points is higher. Poly(BPEA) was treated with trifluoroacetic acid under the same conditions described above. ^{1}H NMR and THF-phase GPC measurements of the resulting product indicate that the structure of the poly(BPEA) was kept without any chain scission reactions on ester linkages. These results indicate that the hydrolysis of the *tert*-butyl ester groups in the branched PtBuAs obtained by SCVCP proceeds selectively to yield characteristic branched PAAs.

Solution Properties of Branched Poly(acrylic acid)s. The solution properties of the branched PAAs in various solvents may be influenced by the branched architectures, molecular weights, and the number of nonpolar BPEA segments in the vicinity of carboxyl groups. For higher γ values ($\gamma > 6$), the hydrolyzed products in the acid form are soluble directly in water (pH $\geq$ 2.5) and methanol, while insoluble in dichloromethane. For the branched PAAs having higher degree of branching ($2.5 \geq \gamma \geq 0.5$), the acid form is soluble in most organic solvents, such as dichloromethane, acetone, and dioxane, while insoluble directly in water, which may be due to the higher composition of the nonpolar BPEA segment in the resulting branched PAAs. These polymers are only soluble in water at high pH (pH > 10), i.e., in the neutralized form.

The solubility of the branched PAAs in water should be closely related to the fraction of charged monomers; that is to say, PAA is virtually undissociated at low pH values, whereas a fully charged chain results at high pH. Hence, it is interesting to know the degree of dissociation, i.e., the charge density of the polymer, when one discusses the solubility as well as the solution behavior at a given pH. Potentiometric titration curves for the representative branched PAAs are shown in Figure 11, where the degree of ionization is plotted against solution pH. In all cases, the pH values increase systematically with increasing the degree of ionization. The apparent pK_a values (taken as the pH at 50% ionization) were determined for the branched PAAs from the titration curves. For the branched PAAs at $\gamma = 10$ and 100 they were found to be p$K_{a,app} = 5.8-6.0$, which is comparable to the corresponding value for linear PAA homopolymers, p$K_{a,app} \approx 5.8$.[41] The branched PAA at $\gamma = 2.5$ become insoluble for pH $\leq$ 4.7. That point corresponds to about 50% ionization, indicating that

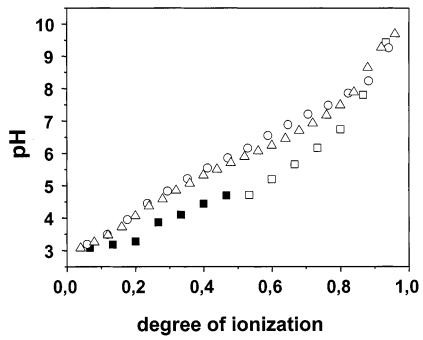

Figure 11. Potentiometric titration curves for branched PAAs: $\gamma = 100$ (○), 10 (△), and 2.5 (□, ■) in aqueous solutions. The filled symbols (■) indicate the region where PAA was insoluble in aqueous solution.

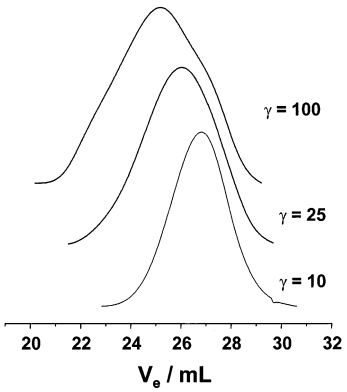

Figure 12. Aqueous-phase GPC traces of the branched PAAs obtained after the hydrolysis.

dissociation of half of the acid function in the branched polymer chains leads to water solubility. For the branched PAAs having higher degree of branching ($\gamma \leq 1.5$), the transition points are at pH > 8, suggesting that these polymers are soluble in water only at high degrees of ionization. In any case, a pH >10 is sufficient to reach the fully dissociated state of the branched PAA chains. It is suggested that the solubility of the branched PAAs is dominated mainly by the composition of PAA in the copolymer as well as increased charge densities in the compact branched structures.

Figure 12 represents aqueous-phase GPC traces of the branched PAAs. All samples show a broad distribution, and the elution curves shift toward higher molecular weights with increasing γ ratio. The same tendency was observed in the THF-phase GPC traces of the branched PtBuAs before hydrolysis. The molecular weights of the branched PAAs, M_{PAA}, can be roughly calculated as

$$M_{PAA} = M_{PtBuA}\frac{m_{AA}\gamma + m_{BPEA}}{m_{tBuA}\gamma + m_{BPEA}} \qquad (3)$$

where m_{tBuA}, m_{AA}, and m_{BPEA} are molar masses of monomers and inimer, respectively. The number- and weight-average molecular weights of PtBuAs obtained from GPC/viscosity were used for the calculation. In all cases, the calculated number-average molecular weights are 1.6−1.8 times higher than the apparent values determined by aqueous-phase GPC using PMAA standards, as can be seen in Table 4. Obviously, these molecular weights are not accurate, due to linear samples used as calibration standards. The relatively broad molecular weight distributions of the branched PAAs ($M_w/M_n = 3-7$) are comparable to those of the

Table 4. Characterization of Water-Soluble Branched Poly(acrylic acid)s

sample[a]	γ[b]	$M_{n,calcd}$[c]	$M_w/M_{n,calcd}$[d]	$M_{n,GPC}$[e]	$M_w/M_{n,GPC}$[e]	R_h (nm)[f] at pH 3	R_h (nm)[f] at pH 10
6	10	14 400	3.52	8 600	2.99	1.7	2.2
7	25	25 900	3.32	14 400	4.48	2.9	4.1
10	100	43 400	4.51	25 000	6.86	3.2	5.2

[a] Branched PtBuA used for the hydrolysis; see Table 1. [b] $\gamma = [tBuA]_0/[BPEA]_0$. [c] $M_{n,calcd} = M_{n,GPC-VISCO}$ of PtBuA $\times$ $(m_{AA}\gamma + m_{BPEA})/(m_{tBuA}\gamma + m_{BPEA})$. [d] $M_w/M_{n,calc.} = M_w/M_{n,GPC-VISCO}$ of PtBuA. [e] Determined by aqueous-phase GPC using linear poly(methacrylic acid) standards. [f] *Z*-average hydrodynamic radius determined by DLS in 0.1 M NaCl aqueous solution.

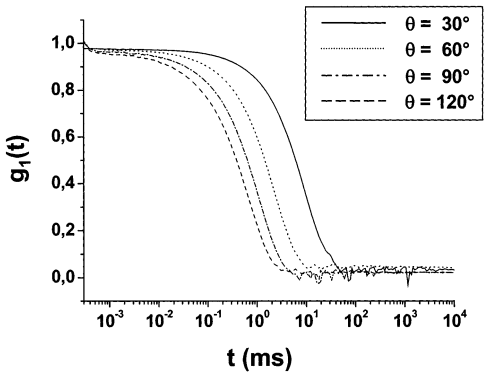

Figure 13. Normalized field correlation functions of the branched PAA ($\gamma = 10$) in 0.1 M NaCl aqueous solution (c = 2.0 mg/mL) at pH 10 at various angles.

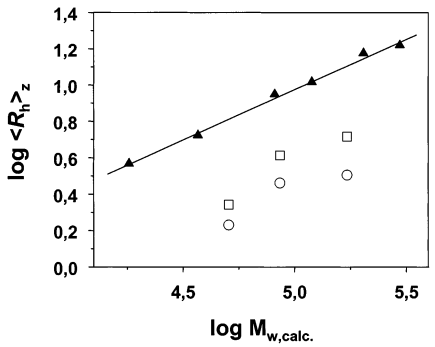

Figure 14. Dependence of average hydrodynamic radius (R_h) on weight-average molecular weight ($M_{w,calc.}$) of the branched PAAs: R_h was measured at pH = 3 (○) and pH = 10 (□). Linear PAAs (▲) at pH = 6−8 used as a reference are derived from Reith et al.[42]

branched PtBuAs. These results suggest that water-soluble branched PAAs with apparent number-average molecular weights between 8000 and 25 000 were obtained by SCVCP, with subsequent hydrolysis, and the molecular weights and the branching architecture of the hydrolyzed products correspond to those of the branched PtBuAs.

Dynamic light scattering (DLS) studies were carried out on the representative branched PAAs in water containing 0.1 M NaCl at a concentration of 2.0 mg/mL at room temperature. In all cases, measurements were conducted at four different angles, as can be seen in Figure 13, and the hydrodynamic radius (R_h) of the species was obtained by extrapolation to $q^2 \rightarrow 0$. The values obtained at pH = 3 and pH = 10 are shown in Table 4. In both cases, the R_h of the branched PAAs increases with increasing γ ratio, which is due to both the increase in the molecular weights and the decrease in the degree of branching. The differences in R_h values obtained at different pHs indicate the influence of the charged state on the chain conformation. At basic pH, the electrostatic repulsion between the carboxylate anions causes the branched polymer chain to adopt an open chain conformation. At low pH, on the other hand, the intrachain association of the hardly dissociated PAA chains causes each chain to collapse into a smaller conformation. The values obtained here seem reasonable on the basis of the comparison with the results of linear PAAs reported recently by Reith et al.[42] The authors have determined the weight-average molecular weight and the *z*-average hydrodynamic radius (R_h) of linear PAA samples in NaCl-containing aqueous solution at pH = 6−8 using static and dynamic light scattering. Figure 14 compares the R_h values of the branched PAAs obtained in this work and the reported values of linear PAAs as a function of M_w. The R_h value of the branched PAA is always smaller than that of linear ones, indicating the compact structures of the branched polyelectrolytes in aqueous solution. To characterize the branched PAAs as polyelectrolytes, we discuss here the R_h values, which correspond to single molecules in aqueous solution. Some peaks attributed to aggregates were observed in our measurement which may be due to the intermolecular interactions between the polyelectrolytes. Note that the conditions of DLS measurements used in this study were within the region where no significant dependence of the R_h on the salt concentration and the polymer concentration was found in the case of linear PAAs.[42] Further studies on this interesting branched polyelectrolytes, such as the influence of branched architectures on the chain configuration in aqueous solution under various salt concentrations and pHs, will be communicated separately.

Conclusions

Self-condensing vinyl copolymerization (SCVCP), followed by hydrolysis, enabled us to synthesize highly branched polyelectrolytes, in which the molecular weights, the composition of the PAA segments, and the branched structures can be adjusted by an appropriate choice of the catalyst system, the comonomer composition, γ, and the polymerization conditions. The close correlation of the bromine content of the branched PtBuAs with the comonomer ratio, γ, indicates that unfavorable termination and transfer are essentially negligible when the CuBr/PMDETA catalyst system is used, and the number of bromoester end groups can be simply manipulated by the ratio, γ. The CuBr/Bipy catalyst system made it possible to produce high molecular weight branched PtBuAs. The significant influence of the polymerization temperature on the resulting products was confirmed on both catalyst systems. It was demonstrated that a suitable choice of the temperature is required to obtain highly branched polymers.

^{1}H NMR, FT-IR, aqueous-phase GPC measurements, and elemental analyses results consistently indicate that hydrolysis of the *tert*-butyl ester groups in the branched PtBuAs proceeds selectively to yield characteristic branched PAAs, and the branched structure is

intact during the hydrolysis. All branched PAAs obtained in this study are soluble in water at high pH, while only the polymers having lower degree of the branching are soluble at low pH. DLS studies at different pH indicate that a marked stretching of the branched chains takes place when going from a virtually uncharged to a highly charged stage. The comparison of the hydrodynamic radius of the branched PAAs and linear ones as a function of M_w suggests that highly compact structures of the polyelectrolytes can be obtained due to their branched architectures. This convenient synthetic approach may lead to further development of branched polyelectrolytes, combined with the detailed investigations of the relation of the chain architectures and the solution properties. Attachment of the highly branched polymers on the flat and spherical surfaces will lead to interesting materials with high charge density on the surfaces.[28,29]

Acknowledgment. D.C.S. (University of Bordeaux I) acknowledges a grant from the Erasmus exchange program. This work was supported by the Deutsche Forschungsgemeinschaft (Schwerpunkt "Polyelektrolyte").

References and Notes

(1) Dautzenberg, H.; Jaeger, W.; Kotz, J.; Philipp, B.; Stscherbina, D. *Polyelectrolytes: Formation, Characterization and Application*; 1994.
(2) Smits, R. G.; Koper, G. J. M.; Mandel, M. *J. Phys. Chem.* **1993**, *97*, 5745−51.
(3) Borkovec, M.; Koper, G. J. M. *Prog. Colloid Polym. Sci.* **1998**, *109*, 142−152.
(4) Smisek, D. L.; Hoagland, D. A. *Science (Washington, D.C.)* **1990**, *248*, 1221−3.
(5) Heinrich, M.; Rawiso, M.; Zilliox, J. G.; Lesieur, P.; Simon, J. P. *Eur. Phys. J. E* **2001**, *4*, 131−42.
(6) Antonietti, M.; Briel, A.; Förster, S. *Macromolecules* **1997**, *30*, 2700−4.
(7) Ding, J.; Chuy, C.; Holdcroft, S. *Chem. Mater.* **2001**, *13*, 2231−3.
(8) Zioga, A.; Sioula, S.; Hadjichristidis, N. *Macromol. Symp.* **2000**, *157*, 239−49.
(9) Pitsikalis, M.; Sioula, S.; Pispas, S.; Hadjichristidis, N.; Cook, D. C.; Li, J.; Mays, J. W. *J. Polym. Sci., Part A: Polym. Chem.* **1999**, *37*, 4337−50.
(10) Hadjichristidis, N.; Pispas, S.; Pitsikalis, M.; Iatrou, H.; Vlahos, C. *Adv. Polym. Sci.* **1999**, *142*, 71−127.
(11) Voulgaris, D.; Tsitsilianis, C.; Grayer, V.; Esselink, F. J.; Hadziioannou, G. *Polymer* **1999**, *40*, 5879−89.
(12) Wu, C.; Ma, R.; Zhou, B.; Shen, J.; Chan, K. K.; Woo, K. F. *Macromolecules* **1996**, *29*, 228−32.
(13) Muthukumar, M. *Macromolecules* **1993**, *26*, 3904−7.
(14) Wolterink, J. K.; Leermakers, F. A. M.; Fleer, G. J.; Koopal, L. K.; Zhulina, E. B.; Borisov, O. V. *Macromolecules* **1999**, *32*, 2365−77.
(15) Borkovec, M.; Koper, G. J. M. *Macromolecules* **1997**, *30*, 2151−8.
(16) Borisov, O. V.; Birshtein, T. M.; Zhulina, E. B. *Prog. Colloid Polym. Sci.* **1992**, *90*, 177−81.
(17) Borisov, O. V.; Zhulina, E. B. *Eur. Phys. J. B* **1998**, *4*, 205−17.
(18) Misra, S.; Mattice, W. L.; Napper, D. H. *Macromolecules* **1994**, *27*, 7090−8.
(19) Held, D.; Müller, A. H. E. *Macromol. Symp.* **2000**, *157*, 225−37.
(20) Simon, P. F. W.; Müller, A. H. E. *Macromolecules* **2001**, *34*, 6206−13.
(21) Cheng, G.; Simon, P. F. W.; Hartenstein, M.; Müller, A. H. E. *Macromol. Rapid Commun.* **2000**, *21*, 846−52.
(22) Schöen, F.; Hartenstein, M.; Müller, A. H. E. *Macromolecules* **2001**, *34*, 5394−7.
(23) Hartenstein, M.; Müller, A. H. E. Manuscript in preparation.
(24) Cheng, G.; Böker, A.; Zhang, M.; Krausch, G.; Müller, A. H. E. *Macromolecules* **2001**, *34*, 6883−8.
(25) Gaynor, S. G.; Edelman, S.; Matyjaszewski, K. *Macromolecules* **1996**, *29*, 1079−81.
(26) Litvinenko, G. I.; Simon, P. F. W.; Müller, A. H. E. *Macromolecules* **2001**, *34*, 2418−26.
(27) Litvinenko, G. I.; Simon, P. F. W.; Müller, A. H. E. *Macromolecules* **1999**, *32*, 2410−9.
(28) Mori, H.; Böker, A.; Krausch, G.; Müller, A. H. E. *Macromolecules* **2001**, *34*, 6871−82.
(29) Mori, H.; Chan Seng, D.; Zhang, M.; Müller, A. H. E. *Langmuir* **2002**, *18*, 3682−93.
(30) Matyjaszewski, K.; Gaynor, S. G.; Kulfan, A.; Podwika, M. *Macromolecules* **1997**, *30*, 5192−4.
(31) Sanayei, R. A.; Suddaby, K. G.; Rudin, A. *Makromol. Chem.* **1993**, *194*, 1953−63.
(32) Radke, W.; Simon, P. F. W.; Müller, A. H. E. *Macromolecules* **1996**, *29*, 4926−30.
(33) Burchard, W. *Adv. Polym. Sci.* **1999**, *143*, 113−94.
(34) Matyjaszewski, K.; Pyun, J.; Gaynor, S. G. *Macromol. Rapid Commun.* **1998**, *19*, 665−70.
(35) Matyjaszewski, K.; Gaynor, S. G.; Müller, A. H. E. *Macromolecules* **1997**, *30*, 7034−41.
(36) Yan, D.; Müller, A. H. E.; Matyjaszewski, K. *Macromolecules* **1997**, *30*, 7024−33.
(37) Coessens, V.; Pyun, J.; Miller, P. J.; Gaynor, S. G.; Matyjaszewski, K. *Macromol. Rapid Commun.* **2000**, *21*, 103−9.
(38) Weimer, M. W.; Fréchet, J. M.; Gitsov, I. *J. Polym. Sci., Part A: Polym. Chem.* **1998**, *36*, 955−70.
(39) Zhang, X.; Chen, Y.; Gong, A.; Chen, C.; Xi, F. *Polym. Int.* **1999**, *48*, 896−900.
(40) Matyjaszewski, K.; Gaynor, S. G. *Macromolecules* **1997**, *30*, 7042−9.
(41) Sato, Y.; Hashidzume, A.; Morishima, Y. *Macromolecules* **2001**, *34*, 6121−30.
(42) Reith, D.; Müller, B.; Müller-Plathe, F.; Wiegand, S. *J. Chem. Phys.* **2002**, *116*, 9100−6.

MA021159U